Journal of Materials Chemistry B

Accepted Manuscript

ROYAL SOCIETY OF CHEMISTRY

www.rsc.org/materialsB

Journal Name

ARTICLE

Multifunctionalized Polyurethane-Polyurea Nanoparticles: Hydrophobically Driven Self-Stratification at the o/w Interface Modulates Encapsulation Stability

Received 00th January 20xx,
Accepted 00th January 20xx

DOI: 10.1039/x0xx00000x

www.rsc.org/

Pau Rocas[a]*, Yolanda Fernández[b], Simó Schwartz Jr[b], Ibane Abasolo[b], Josep Rocas[c]*, Fernando Albericio[d]*

Polyurethane-Polyurea (PUUa) reactive prepolymers with adjusted hydrophobic and hydrophilic dangling chains to achieve multiwalled sub-30 nm nanoparticles are presented. The combination of an amphiphilic and a hydrophobic prepolymer in the oil-in-water interface creates a stratified shell by hydrophobic interactions. These novel nanostructures enhance the encapsulation stability of lipophilic compounds compared to monowalled nanostructures and facilitate the selective and ordered functionalization along the multiwalled shell with bioactive motifs. As proof of concept, PUUa nanoparticles have been engineered with disulfide bonds and an αvβ3 integrin-selective cyclic RGD peptide (cRGDfK) providing our system with glutathione (GSH) triggered controlled release and cell targeting specificity to U87 tumor cells, respectively.

1. Introduction

Merging cross-functional fields as chemistry, engineering, medicine, and biology to achieve multifunctional stimuli responsive drug delivery systems (DDS) is one of the major challenges in modern medicine[1,2]. Therefore, large efforts are being undertaken to unravel the unknowns which provoke that even today an *in vivo* reliable and efficient smart nano-system has not been completely achieved. Obviously, in the past decade, great progress has been made in the creation of advanced DDS, although, these are usually formed through the emulsification of a hydrophobic drug in water using external surfactants[3,4]. Unwillingly, this kind of DDS commonly lack chemical tailorability, encapsulation efficiency, targeting selectivity, biocompatibility and controlled degradability, among others. One recurrent issue in top used multiblock polymeric systems like PLA, PLGA, PMMA, etc. is the lack of reactive sites that enable multifunctionality. So, smarter nano-systems with complex structures such as dendrimers or multibranched polymers arose. Sadly, sometimes the difficult syntheses, sometimes the costly purification steps limited their industrial and commercial translation. Accordingly, nanoparticles (NPs) fulfilling these structural, delivery and biological requirements are needed in the demanding field of nanomedicine. The scientific community is nowadays highly concerned with the possibility to achieve not only multifunctionality but also self-assembled nanostructured architectures for multiple purposes[5,6]. Concretely, the capacity of polymers to be self-structured forming the shell of a nano-system is directly related to the ease with which their molecular structure can be modified. So, the tailored design of a polymer is only viable when it is not only chemically tunable but also cost-efficient[7,8]. Thus, to get structural control at the nano-level, a different kind of prepolymers with adjustable physico-chemical and bioactive characteristics is needed. Therefore, polyurethanes and polyureas constitute a potential choice to fulfill such needs. In this aspect, very few publications have reported on the application of reactive polymeric surfactants containing free isocyanate groups[9–11]. The high reactivity of isocyanates with hydroxyl and/or amine containing precursors allow a fast structure stabilization by crosslinking and an efficient functionalization of micro and nanoparticles via polyurethane and/or polyurea bonds. Specifically, PUUa diisocyanate prepolymers can create stable shells by anchoring a wide range of nucleophile-containing (amines, thiols, alcohols, etc.) bioactives[12]. In example, polyisocyanates with high functionality (f>2) allow multiple bonding of bioactive molecules that confer targeting properties and at the same time modulation of their intrinsic hydrophilic-lipophilic balance[13,14]. Of note, to ensure a good biocompatibility and reduce toxicity of biodegraded products aliphatic isocyanates need to be selected instead of aromatic ones[15–17]. Since the late sixties their biocompatibility for

[a,d] Institute for Research in Biomedicine (IRB Barcelona), Baldiri Reixac 10, 08028 Barcelona Spain

[c] Nanobiotechnological Polymers Division, Ecopol Tech S.L., Indústria 7, 43720 L'Arboç, Tarragona, Spain

[d] Department of Organic Chemistry, University of Barcelona, Martí Franquès 1-11, 08028 Barcelona, Spain

School of Chemistry & Physics, University of Kwazulu-Natal, 4041 Durban, South Africa

[b] CIBBIM-Nanomedicine, VHIR Vall d'Hebron Institut de Recerca, 08035 Barcelona, Spain

[b,d] CIBER-BBN, Networking Centre on Bioengineering Biomaterials and Nanomedicine, 08028 Barcelona, Spain

biomedical use has been well proven as it is one of the materials of choice in clinical use for development of catheters, stents, valves, etc. The quantitative synthetic procedures, facile scalable processes and broad chemistry of PUUa opens an infinite range of potential incorporation of functionalities. Multiple chemical complexities, biodegradation, targeting and biocompatibility are some of the clear advantages that PUUa polymers can bring to the table as future smart and nanostructured DDS.

Herein we depict the combination of two PUUa prepolymers (one amphiphilic and the other hydrophobic) in aqueous media to create hydrophobically ordered shells. That novel prepolymers contain dangling chains of sharply different polarity to promote a controlled stratification in the oil-water interface to achieve multiwalled nanostructures and bear terminal isocyanate groups for a final crosslinking step to "freeze" the preformed architecture. These nanostructures are designed to improve the encapsulation stability of hydrophobic cargos providing a deeper encapsulation in the NP core compared to monowalled nanostructures where cargos are closer to the shell surface and burstly-released under *in vivo* conditions[18].

2. Materials and methods

2.1. Chemicals

Cyclo(-Arg-Gly-Asp-D-Phe-Lys) (cRGDfK) was synthesized in house according to previously reported protocols[19]. YMER N-120 was kindly provided by Perstorp (Perstorp, Sweden) and N-Coco-1,3-propylenediamine (Genamin TAP 100D) by Clariant (Barcelona, Spain). Capric/caprylic triglyceride mixture (Crodamol GTCC) was obtained from Croda (Barcelona, Spain) and Bayhydur 3100 was purchased from Bayer (Leverkusen, Germany). If not indicated otherwise, all other reagents were purchased from Sigma-Aldrich (St Louis, MO, USA). Extra dry acetone was used during all the synthetic process.

2.2. Cell lines and cell culture

Human glioblastoma cell line (U87-MG) and human colorectal cancer cell line (HT-29) used in cell internalization assays and human cervix carcinoma cell line (HeLa) used in cytotoxicity assays were obtained from the American Type Culture Collection. All cell lines were maintained as recommended. Briefly, U87-MG cells were maintained in DMEM medium and HT-29 and HeLa cells in RPMI 1640 medium, both from Life Technologies. All media were supplemented with 10% heat-inactivated fetal bovine serum (FBS) (56 °C, 30 min), penicillin (100 U/mL), streptomycin (100 µg/mL) and Fungizone (250 ng/mL) (Life Technologies, Madrid, Spain). Cells were maintained in a humid atmosphere at 37 °C with 5% CO_2.

2.3. Experimental methods

2.3.1. Synthesis of reactive prepolymers for Multiwalled PUUa NPs preparation

2.3.1.1. Preparation of the reactive amphiphilic prepolymer (Amphil).

To synthesize the amphiphilic prepolymer, a 500 mL four-necked reaction vessel was pre-heated at 50 ºC and purged with nitrogen. Then, YMER N-120 (5.50 g, 5.5 mmol), 2-Hydroxyethyl disulfide (DEDS) (0.15 g, 1 mmol), Crodamol GTCC (0.75 g) and IPDI (3.38 g, 15 mmol) were added to the reaction vessel under mechanical stirring with dibutyltin dilaurate (DBTL) as catalyst (3 mg, 4.65 µmol). The polyaddition reaction was maintained in these conditions until DEDS and YMER reacted quantitatively with IPDI as ensured by FT-IR (Fig. S5) and automatic titration[20] (Fig. S2). At this point, the vessel was cooled to 40 ºC and Genamin TAP 100D (1.45 g, 4.44 mmol) dissolved in 10 g of acetone was added under constant stirring and left to react for 30 min (Fig. S1). The formation of polyurethane and polyurethane-polyurea prepolymers was followed by automatic titration (Fig. S2) and FT-IR (Fig. S5) and characterized by NMR[21] (Fig. S7).

2.3.1.2. Preparation of the reactive hydrophobic prepolymer (Hyfob).

To synthesize the hydrophobic prepolymer, a schlenk flask of 20 mL was pre-heated at 50ºC and purged with nitrogen. Then, DEDS (0.15 g, 1 mmol) and IPDI (0.485 g, 2.18 mmol) in acetone (7 g) were added with DBTL as catalyst (0.24 mg, 0.37 µmol) and left to react during 1 h with magnetic stirring. At this point, the Schlenk flask was cooled to 40 ºC and Genamin TAP 100D (0.15 g, 0.5 mmol) in 3 g acetone was added under constant stirring and left to react for 30 min (Fig. S1). The formation of polyurethane and polyurethane-polyurea prepolymers was followed by FT-IR (Fig. S4) and and characterized by NMR[21] (Fig. S7).

2.3.1.3. Preparation of Bayhydur 3100-cRGDfK conjugate (B3100-cRGDfK).

The peptide cRGDfK (36 mg, 0.0596 mmol) was dissolved in phosphate buffered saline (PBS) (1 mL, 5ºC) and 10 µL of pure triethylamine were added to the mixture (pH 10). Then, the previous solution was mixed with Bayhydur 3100 linker (B3100) (125 mg, 0.167 mmol) and allowed to react during 2 h at 5ºC under constant stirring (Fig. S1). The bonding of one cRGDfK molecule per B3100 linker, the reaction kinetics between cRGDfK and B3100, and the total concentration of linked cRGDfK in PUUa NP-RGD was ensured by MALDI-TOF MS (Fig. S9) and HPLC (Fig. S10 and Table S1), respectively.

2.3.2. Synthesis of Multiwalled polyurethane-polyurea nanoparticles.

2.3.2.1. PUUa NPs synthesis.

A previously homogenized aliquote of Amphil+Hyfob (1.69 g, mass ratio Amphil 13.35:1 Hyfob) (see section 2.3.1.) was added in a round-bottom flask containing B3100 (125 mg, 0.167 mmol) under nitrogen atmosphere. This organic mixture was then emulsified in PBS (16 mL, pH 7.4, 5ºC) in a magnetic stirrer under an ice bath to prevent isocyanate reaction with water. Once emulsified, L-lysine was added (68.56 mg, 0.47 mmol) and the interfacial polyaddition reaction was controlled by FT-IR. After 30 min, DETA (32.18 mg, 0.31 mmol) was added and the crosslinked nanoparticles were formed by a second interfacial polyaddition as proved by FT-IR. Acetone was mildly removed in the rotavapor. PUUa NPs were dialysed (100000 MWCO, Spectrum Laboratories, California, USA) against pure water during 72 h for Zeta potential experiments. For in vitro experiments PUUa NPs were dialysed against PBS during 72 hours.

2.3.2.2. PUUa DiI loaded NPs synthesis (PUUa NP-DiI).

These NPs were synthesized as previously described (see section 2.3.2.1.) adding Amphil+Hyfob in a round bottom flask containing DiI (2.5 mg, 2.67 µmol) as fluorophore. The organic mixture was homogenized and subsequently, section 2.3.2.1 followed without modifications.

2.3.2.3. PUUa DiO loaded NPs synthesis (PUUa NP-DiO).

These NPs were synthesized as previously described (see section 2.3.2.2.) using DiO (2.5 mg, 2.83 µmol) as fluorophore instead of DiI.

2.3.2.4. All-in-one PUUa NPs formation (PUUa NP-DiI-RGD).

These PUUa NPs were synthesized as previously described (see section 2.3.2.1.) using B3100-cRGDfK as targeting conjugate. Amphil+Hyfob organic mixture was mixed with the previously described B3100-cRGDfK conjugate solution (see section 2.3.1.3.) (16 % w/w) followed by emulsification in PBS (16 mL, pH 7.4, 5ºC) in a magnetic stirrer under an ice bath to prevent isocyanate reaction with water. At this point, section 2.2.1. was followed without modifications.

2.3.2.5. PUUa NPs DETA crosslinked

Section 2.3.2.1. was followed but crosslinked by interfacial polyaddition only with DETA (64.36 mg, 0.62 mmol).

2.3.2.6. PUUa NPs Lys crosslinked

Section 2.3.2.1. was followed but crosslinked by interfacial polyaddition only with L-lysine (137.12 mg, 0.94 mmol).

2.3.3 Synthesis of reactive prepolymer for Monowalled PUUa NPs preparation

2.3.3.1. Preparation of the reactive amphiphilic prepolymer (Amphil).

To allow a logical comparison between nanoparticles, monowalled ones contained the same total amount of monomers than multiwalled ones but just in one Amphil prepolymer. To synthesize the amphiphilic prepolymer, a 500 mL four-necked reaction vessel was pre-heated at 50 ºC and purged with nitrogen. Then, YMER N-120 (5.50 g, 5.5 mmol), 2-Hydroxyethyl disulfide (DEDS) (0.30 g, 2 mmol), Crodamol GTCC (0.75 g) and IPDI (3.866 g, 17 mmol) were added to the reaction vessel under mechanical stirring with dibutyltin dilaurate (DBTL) as catalyst (3.24 mg, 5.02 µmol). The polyaddition reaction was maintained in these conditions until DEDS and YMER reacted quantitatively with IPDI as ensured by FT-IR and automatic titration[20]. At this point, the vessel was cooled to 40 ºC and Genamin TAP 100D (1.6 g, 4.94 mmol) dissolved in 10 g of acetone was added under constant stirring and left to react for 30 min. The formation of polyurethane and polyurethane-polyurea prepolymers was followed by FT-IR.

2.3.4. Synthesis of Monowalled polyurethane-polyurea nanoparticles

2.3.4.1. PUUa DiI loaded NPs synthesis (PUUa NP-DiI).

A previously homogenized aliquote of Amphil (1.69 g) (see section 2.3) was added in a round-bottom flask containing DiI (2.5 mg, 2.67 µmol) as fluorophore and B3100 (125 mg, 0.167 mmol) under nitrogen atmosphere. This organic mixture was then emulsified in PBS (16 mL, pH 7.4, 5ºC) in a magnetic stirrer under an ice bath to prevent isocyanate reaction with water. Once emulsified, L-lysine was added (68.56 mg, 0.47 mmol) and the interfacial polyaddition reaction was controlled by FT-IR. After 30 min, DETA (32.18 mg, 0.31 mmol) was added and the crosslinked nanoparticles were formed by a second interfacial polyaddition as proved by FT-IR. Acetone was mildly removed in the rotavapor. PUUa NPs were dialysed (100000 MWCO, Spectrum Laboratories, California, USA) against pure water during 72 h for FRET experiments.

2.3.4.2. PUUa DiO loaded NPs synthesis (PUUa NP-DiO).

These NPs were synthesized as previously described (see section 2.3.4.1.) using DiO (2.5 mg, 2.83 µmol) as fluorophore instead of DiI.

2.4. Analytical techniques

2.4.1. Transmission electron microscopy. The nanoparticles morphology was studied in a Jeol JEM 1010 (Peabody, MA, USA). A 200 mesh copper grid 0,75% FORMVAR coated was deposited on a drop of 10 mg/mL of nanoparticles in water during 1 min. Nanoparticles excess was removed by fresh milliQ water contact for 1 min. Then, the grid was deposited on a drop of Uranyl acetate 2 % w/w in water for 30 sec. The Uranyl acetate excess was blotted off and air-dried before measurement. For the degradation experiment, 10 µL of filtered (0,22 µm) PUUa NPs (100mg/mL) were added into 1 mL solution of GSH (10 mM) and incubated at 37 ºC during 24 h under constant stirring. For statistical analysis, 5 different zones of the copper grid were randomly counted with ImageJ software (NIH, Bethesda, MD, USA).

2.4.2. B3100-cRGDfK reaction control. The reaction solution containing B3100 and cRGDfK (see section 2.1.3.) was analysed at 0 and 2 hours of reaction. Analytical HPLC runs of B3100-cRGDfK were performed in a WATERS 2998 HPLC (Milford, MA, USA) using a X-Bridge BEH130, C18, 3.5 µm, 4.6 X 100 mm reverse phase column with the following gradient: 5-15% B in 9 min at a flow rate of 1 mL/min; eluent A: H2O with 0.045% TFA (v/v); eluent B: CH3CN with 0.036% TFA.

2.4.3. PUUa NP-RGD conjugation yield quantification. A calibration curve was performed by preparing 5 standard solutions of cRGDfK peptide containing L-phenylalanine amide as internal standard for quantitative HPLC analysis. Analytical HPLC runs of the PUUa NP-RGD were performed in a WATERS 2998 HPLC (Milford, MA, USA) using a X-Bridge BEH130, C18, 3.5 µm, 4.6 X 100 mm reverse phase column with the following gradient: 5-30% B in 9 min at a flow rate of 1 mL/min; eluent A: H2O with 0.045% TFA (v/v); eluent B: CH3CN with 0.036% TFA.

2.4.4. Size distribution by DLS. PUUa NP and PUUa NP-RGD were analysed on a Malvern Zetasizer Nano-ZS90 (Malvern, UK) at 1 mg/mL in pure water at 37 ºC.

2.4.5. Zeta Potential measurements. PUUa NP and PUUa NP-RGD were analysed on a Malvern Zetasizer Nano-ZS90 (Malvern, UK) at 20 mg/mL in pure water at 37 ºC.

2.4.6. Infrared spectra. IR spectra were performed in a FT-IR Nexus Termo Nicolet 760 (Waltham, MA, USA) by depositing a drop of previously dissolved prepolymer at 1 % in acetone on a NaCl or BaF_2 (for aqueous samples) disk.

2.4.7. Automatic titration. Prepolymer sample after dissolved in dry toluene reacted with excessive di-n-Butylamine standard, and residual di-n-Butylamine was back-titrated with 1M hydrochloric acid up to the endpoint. The content of Isocyanate was calculated from titration volume.

2.4.8. FRET experiments.

Control experiment. To evaluate the kinetics of hydrophobic molecules leakage, 10 µL of 100 mg/mL PUUa NP containing DiI (0.15 mg/mL) and 10 µL of 100 mg/mL PUUa NP containing DiO (0.15 mg /mL) were diluted to 1 mL pure fresh water. Experiments in spectrofluorimeter Varian Cary Eclipse (Palo Alto, CA, USA) were carried out by excitation of the donor at 470 nm and measuring the

emission from 480 to 650 nm with constant magnetic stirring at 37 ºC during 24 h.

GSH experiment. The same experiment was repeated adding the needed mg of GSH in the cell to be at 10 mM after 3 h of experiment.

PC-Chol liposomes experiment. The same experiment was repeated adding 10 µL of 100 mg/mL PUUa NP containing DiI (0.15 mg /mL) and 10 µL of 100 mg/mL PUUa NP containing DiO (0.15 mg /mL) to a 1 mL, 10 mM solution of PC-Chol liposomes previously filtered under 0.45 µm.

2.4.9. MALDI-TOF MS. B3100-cRGDfK conjugate formation was ensured by MALDI-TOF MS. The experiment was carried out on an Applied Biosystems Voyager-DETMRP mass spetrometer (Waltham, MA, USA), using α-cyano-4-hydroxycinnamic acid (ACH) as matrix. B3100 and B3100-cRGDfK at 1 mg/mL after 2 h reaction were analysed.

2.4.10. NMR. NMR spectra were recorded on a Varian Mercury (400 MHz) (Agilent) (Santa Clara, CA, USA). Reactive prepolymers Hyfil, Amphil and Hyfob were previously dissolved in $CDCl_3$ at 100 mg/mL.

2.4.11. Lyophilization and redispersion procedures. Previously dialysed samples (100 mg/mL) were lyophilized and directly redispersed at the desired concentration by overnight stirring at 1500 rpm. Lyophilized and redispersed samples were examined by TEM and DLS to ratify optimal size and morphology characteristics.

2.5. Biological studies

2.5.1. Integrin expression characterization. Expression of $\alpha_V\beta_3$ and $\alpha_V\beta_5$ was analyzed by flow cytometry using monoclonal antibodies against both heterodimers (MAB1976H and MAB1961F from Millipore). Precisely, cell suspensions deattached using PBS-EDTA (5mM) were incubated with 3 µg of $\alpha_V\beta_3$ antibody and 1 µg of $\alpha_V\beta5$ antibody during 20 min at 4ºC. IgG2 isotype controls from eBioscience (San Diego, CA, USA) were included. Cells were analyzed using FacScalibur Becton Dickinson (Franklin Lakes, NJ, USA) and FCS Express 4 software De Novo Software (Los Angeles, CA, USA).

2.5.2. Cell internalization by flow cytometry. Time dependent internalization of targeted and non-targeted PUUa NPs was studied by flow cytometry. Precisely, exponentially growing cultures were detached using PBS-EDTA (5 mM), resuspended in Ca^{2+} and Mg^{2+} free PBS and incubated at 37ºC with a final concentration of 38.5 µg/mL of NPs containing 10 µg/mL of DiI. After the incubation, cells were washed twice with PBS and stained with DAPI (50 µg/mL) to include only viable cells into the analysis. Cells were analyzed using LRS Fortessa Becton Dickinson (Franklin Lakes, NJ, USA) and FCS Express 4 software De Novo Software (Los Angeles, CA, USA).

2.5.3. Cell internalization and lysosomal colocalization by confocal microscopy. Cells were seeded in 24 well-plates containing coverslips (50,000 cells/well) and left overnight at 37 °C with 5% CO_2 to allow cell attachment. Cells were then washed carefully with PBS and 1 µg/mL of DiI containing PUUa NPs (with or without RGD targeting moieties) were added to the cultures diluted in complete cell growing media. After the incubation period, cells were washed twice with PBS and stained 15 min with 10 µM of Lysotracker Green (Life Technologies) and directly visualized using confocal microscope (FV1000, Olympus). Confocal images of the same Z plane were obtained for Lysotracker (green signal) and for DiI (red signal), using excitation peaks at 488/561 nm and emission at 522/585 nm for Lysotracker and DiI, respectively and merged afterwards to demonstrate that some of the nanoparticles are allocated inside acidic organelles labeled by Lysotracker. Images were acquired at 60x magnification. Quantification of the NP signal outside the lysosomes was performed using Fiji ImageJ[22] (NIH, Bethesda, MD, USA) in confocal images taken from at least three different fields. Red signal in every cell in each field (8-14) was quantified for each z-plane, and then compared statistically using the *t*-student test with GraphPad software (La Jolla, CA, USA).

Cytotoxicity studies. In vitro cytotoxicity of NPs was tested by 3-[4,5-dimethylthiazol-2-yl]-2,5-diphenyltetrazolium bromide (MTT) method after 72 h incubation[23]

3. Results and discussion

As we have shown in our recent methodological patent many nanoparticles with multiple structural and biological functionalities can be obtained due to the versatile polyurethane chemistry. In fact, the novel kind of NPs based on reactive polyurethane and polyurea prepolymers introduced herein allowed controlled stratification at the nano-interface and tunable functionality in their multiwalled structure[24] (Fig. 1a and 1b). As proof of concept for cancer therapy, disulfide bonds were successfully included in the prepolymers to enable a tailored degradation and a controlled intracellular release of encapsulated hydrophobic molecules at intracellular GSH concentration. Moreover, a cyclic hydrophilic RGD peptide located on the outer shell of the NP was selected and innovatively conjugated to mediate specific targeting to cells overexpressing αvβ3 integrin (Fig. 1c). Finally, to strengthen this stratified structure a crosslinking step with polyamines was key to form an isocyanate-free, ordered and robust nanostructure[25–27].

Thus, we synthesized two new reactive prepolymers by successive quantitative polyaddition reactions of difunctional monomers with an aliphatic diisocyanate (Isophorone diisocyanate) (see monomers description in the ESI and Fig. S1 and Table S1) and characterized them by automatic titration (Fig. S2), FT-IR (Fig. S3 and Fig. S4) and NMR (Fig. S5 and Fig. S6 in the ESI). On one hand, the reactive amphiphilic prepolymer (Amphil) contained disulfide bonds (2-Hydroxyethyl disulfide) in the main chain, hydrophilic (polyethylene glycol monomethyl ether) and hydrophobic (N-Coco-1,3-propylenediamine) dangling side-chains and terminal isocyanate groups. The hydrophilic side-chains self-oriented toward the aqueous surrounding media and emulsifed in water the whole pre-formed PUUa NP. The hydrophobic chains stabilized and encapsulated the inner hydrophobic prepolymer (Hyfob, see below) and the oily core by hydrophobic interactions. Thus, Amphil worked as an all-in-one polymer ensuring oil and water miscibility, redox-degradability and isocyanate reactivity. On the other hand, the hydrophobic reactive prepolymer (Hyfob) bore disulfide bonds in the main chain, terminal isocyanate groups and just hydrophobic dangling side-chains. The idea to introduce a Hyfob in the shell was based on the wish to prevent premature leakage of the encapsulate without renouncing to redox-degradability. In this regard, to achieve this hydrophobically stratified structure, it was also crucial to use a 5% (w/w) of an ultrahydrophobe as core material, such as the biocompatible capric-caprylic triglyceride (Crodamol GTCC). Its solubilizing effect of hydrophobic therapeutically active molecules[28] and ability to decrease coacervation of oily core nanoparticles due

to Ostwald Ripening effect[29] made it the product of choice. In addition, as introduced previously, to convert these hydrophobically driven self- stratified structures into covalently stable isocyanate-free PUUa NPs, the reactive polymeric shell was crosslinked with small polyamines (Fig. S7 in the ESI). Hence, as seen from figure 3 we observed that addition of L-Lysine (Lys), a diaminocarboxylate moiety, into the emulsified reactive prepolymers as pre-crosslinker and extender, reduced the NP size as a result of the enhanced internal emulsifying effect of carboxylate rest[30,31] compared to NPs carrying only polyethylene glycol monomethyl ether (YMER N-120) as hydrophilic precursor. Finally, in any of the formulations the shell was consolidated by a highly reactive small triamine, diethylenetriamine (DETA) (Fig. S8 in the ESI prove isocyanates disappearance by FT-IR after crosslinking reaction).

At this point, with the aim of conferring to our system cell targeting specificity, a novel method was developed to anchor the broadly used hydrophilic cRGDfK cyclic pentapeptide to our PUUa NPs via urea linkage without loss of bioactivity[32]. Concretely, Bayhydur 3100 hydrophilic polyisocyanate linker[33] (B3100) and the cRGDfK free primary amino group of Lys residue were effectively coupled in aqueous media (pH 10, 5 ºC) (Fig. S9 in the ESI). By optimizing the reaction stoichiometry we were able to maintain free NCO moieties in the conjugate for further PUUa NP functionalization with only one peptide per linker molecule, as ensured by MALDI-TOF MS experiments (Fig. S10 in the ESI). Furthermore, the PUUa NP functionalization with B3100-cRGDfK conjugate (PUUa NP-RGD) occurred in a high yield (98.5 %), as quantified by HPLC calibration curve (Table S2 in the ESI). Then, B3100-cRGDfK isocyanate reactive conjugate was fixed in the prepolymeric shell via the previously explained crosslinking step yielding around 2 % cRGDfK per PUUa NP. Transmission Electron Microscopy (TEM) and Dynamic Light Scattering (DLS) revealed monomodal size distributions of about 20 nm for PUUa NP-DiI and PUUa NP-DiI-RGD (Fig. 2a and Fig. 2b). Zeta Potential (Zpot) measurements of dialysis-purified nanoparticles exhibited similar slightly negative surface charges due to the Lys carboxylate (Fig. 2e). This experimental result further corroborated that the hydrophilic character of Lys located him in the outer part of the shell thus proving the self-stratified nanostructure by hydrophobic interactions. In addition, the multiwalled nanoparticles robust structure and hydrophilic surface made them lyophilizable and redispersable in aqueous media without cryoprotectants‡.

Shell biodegradability and specific cargo release are fundamental features in drug delivery systems. To this end, the presence of disulfide bonds in the shell facilitated polymer degradation by reductive enzymes and peptides overexpressed in the cytosolic environment of tumor cells[34]. Concretely, reduced glutathione has an intracellular concentration of 2–10 mM in the cytosol while the extracellular concentration is about 2–20 µM. Taking profit of this intracellular concentration, PUUa NPs degradation and cargo release under reductive conditions were studied by transmission electron microscopy (TEM) and Förster resonance energy transfer (FRET) techniques, respectively. Thus, NPs degradation was determined by TEM before and after a 24 h treatment with 10 mM GSH. Significant differences in size were detected due to polymer aggregates formation after redox-triggered degradation (Fig. 2c and Fig. 2d). To confirm the differences on the release properties of multiwalled and monowalled nanostructures, first, monowalled NPs were morphologically characterized by TEM (Fig. S11) and then, FRET experiments where performed in different media. Thus, we encapsulated two typical cell membrane staining agents[35] as fluorescent lipophilic cargos, namely DiI and DiO, in separate PUUa NPs. As already described by FRET mechanism, changes in fluorophores proximity allowed us to evaluate the release dynamics and potential leakiness of different PUUa NPs[36]. So, both fluorescent probes were encapsulated at a total concentration of 0.15 % w/w to avoid static quenching[37] (Encapsulation efficiency 100 %, Data not shown). PUUa NP-DiI and PUUa NP-DiO were then mixed (FRET PUUa NPs) and the FRET ratio was represented against time as $I_a/(I_d+ I_a)$, where I_a was the maximum intensity of the acceptor and I_d the maximum intensity of the donor. The slope of the linear fit was defined as the release coefficient at 37 ºC for the first 10 h of the experiment (Fig. S13 in the ESI). For both multiwalled and monowalled NPs the release coefficient appeared to be almost negligible in water (0.001 h^{-1} and 0.0001 h^{-1} respectively), which corroborated their outstanding encapsulation stability. Further, as PUUa NPs are expected to stably encapsulate the lipophilic drug until reaching the cytosol of the tumor cell, we wanted to ratify that the cargo would not be released unspecifically during cell internalization. With this in mind, we sought to mimic a cellular microenvironment by mixing egg phosphatidylcholine-cholesterol previously reported liposomes (Lipos)[38] (2:1 w/w) to our FRET PUUa NPs (10 mM). Confirming our expectations, multiwalled NPs were stable during the first 10 h (0.001 h^{-1}), but monowalled NPs exhibited a pronounced increase of the FRET ratio upon mixing with Lipos (0.007 h^{-1}) due to unspecific release. Additionally, under treatment with 10 mM GSH, multiwalled PUUa NPs clearly showed a FRET increase (0.01 h^{-1}) caused by disulfide bonds cleavage and sudden release and mixing of the fluorophores (See Fig. 2f and Fig. S12 in the ESI).

In a final proof of principle study, we first tested that PUUa NPs were not cytotoxic to cells (Fig. S14 in the ESI) and then internalization assays were performed. To that end, PUUa NPs were incubated with HT-29 and U87-MG cancer cells, known to have very low and high expression of αvβ3 integrins, respectively (Table S2). Flow cytometry and confocal studies revealed that, due to the RGD outer localization in the multiwalled structure, PUUa NP-RGD encapsulating DiI fluorophore (PUUa NP-DiI-RGD) entered αvβ3 integrin expressing cells more efficiently (Fig. 4a) than non-functionalized ones. Moreover, internalization of PUUa NP-DiI-RGD in αvβ3-negative HT-29 cells was similar to non-targeted NP, indicating that the enhanced uptake of cRGDfK functionalized NPs observed in U87-MG cells was specific.

Confocal images also showed colocalization of NPs with lysosomal markers (Lysotracker Green), confirming that NPs entered cells through the endocytic pathway, and that the uptake and the lysosomal colocalization was clearly enhanced in the case of PUUa NP-DiI-RGD (Fig. 4b). In order to trace the final cytosolic release of the NPs cargo, U87-MG cells were incubated 1 h with PUUa NP-DiI-RGD washed thoroughly and observed immediately and 24 h later. The initially observed distinctive punctuated signal corresponding to the lysosomal localization changed to a more diffuse uniform fluorescent cell cytoplasm distribution, which, in line with abovementioned FRET experiments proved that our system was able to escape from the lysosome and spread their cargo through the cytosol (Fig. S15 in the ESI).

In conclusion, we have depicted a novel methodology to develop self-stratified PUUa NPs based on the amphiphilic properties of the

different designed pre-polymers, and we have clearly evidenced the better encapsulation ability of multiwalled NPs compared to their monowalled counterparts. This multiwalled structure has been experimentally proved by FRET studies, Zpotential measurements and cell internalization experiments. The use of L-Lysine as extender or pre-crosslinker modulated the size of the micelles reaching very small entities that finally were stabilized by crosslinking with DETA. Cargo delivery and nanoparticle shell degradability were also controlled by incorporating DEDS, a redox moiety that responded to intracellular glutathione. The use of a specifically designed reactive conjugate containing a hydrophilic RGD peptide ensured the straightforward functionalization of the outer part of the nanoparticles shell. These systems convey a multiwalled nanostructure with on-demand release properties and cancer cell targeting behavior. This confirms our PUUa NPs as outstanding platforms for smart drug delivery and opens up a new era in nanostructured systems with multiple targeting and degradation possibilities that generate an enormous range of application opportunities. New characterization techniques are being explored to visually proof the sub-30 nm self-stratified structures. Biological studies with a variety of antitumor drugs are also underway.

Acknowledgements

We gratefully acknowledge MICINN and FEDER (IPT-090000-2010-0001), CICYT (CTQ2012-30930) and the Generalitat de Catalunya (2009SGR 1024).

Notes and references

‡ All data presented belongs to experiments performed with lyophilized and redispersed multiwalled PUUa NPs (For more details see section 3 in supporting information).

1 V. P. Torchilin, *Nat. Rev. Drug Discov.*, 2014, **13**, 813–827.

2 N. Kamaly, Z. Xiao, P. M. Valencia, A. F. Radovic-Moreno and O. C. Farokhzad, *Chem. Soc. Rev.*, 2012, **41**, 2971–3010.

3 K. Landfester, *Angew. Chemie Int. Ed.*, 2009, **48**, 4488–4507.

4 F. Tiarks, K. Landfester and M. Antonietti, *Langmuir*, 2001, **17**, 908–918.

5 L. Wu and J. Baghdachi, *Functional Polymer Coatings: Principles, Methods, and Applications*, WILEY-VCH Verlag GmbH, 2015.

6 Z. Zhang, R. L. Marson, Z. Ge, S. C. Glotzer and P. X. Ma, *Adv. Mater.*, 2015, **27**, 3947–52.

7 D. K. Chattopadhyay and K. V. S. N. Raju, *Prog. Polym. Sci.*, 2007, **32**, 352–418.

8 J. Y. Cherng, T. Y. Hou, M. F. Shih, H. Talsma and W. E. Hennink, *Int. J. Pharm.*, 2013, **450**, 145–162.

9 B. K. Kim and J. C. Lee, *Polymer (Guildf).*, 1996, **37**, 469–475.

10 S.-H. Son, H.-J. Lee and J.-H. Kim, *Colloids Surfaces A Physicochem. Eng. Asp.*, 1998, **133**, 295–301.

11 Heming, A. M.; Mulqueen, P. J.; Scher, H. B.; Shirley, I. M. Use of Reactive Polymeric Surfactants in the Formation of Emulsions, US7199185 B2, 2002, PCT/GB2002/002744, 2002.

12 J. Andrieu, N. Kotman, M. Maier, V. Mailänder, W. S. L. Strauss, C. K. Weiss and K. Landfester, *Macromol. Rapid Commun.*, 2012, **33**, 248–53.

13 M. Ding, N. Song, X. He, J. Li, L. Zhou, H. Tan, Q. Fu and Q. Gu, *ACS Nano*, 2013, **7**, 1918–28.

14 U. Paiphansiri, J. Dausend, A. Musyanovych, V. Mailänder and K. Landfester, *Macromol. Biosci.*, 2009, **9**, 575–84.

15 S. A. Guelcher, *Tissue Eng. Part B. Rev.*, 2008, **14**, 3–17.

16 L. T. Budnik, D. Nowak, R. Merget, C. Lemiere and X. Baur, *J. Occup. Med. Toxicol.*, 2011, **6**, 9.

17 S. A. Guelcher, K. M. Gallagher, J. E. Didier, D. B. Klinedinst, J. S. Doctor, A. S. Goldstein, G. L. Wilkes, E. J. Beckman and J. O. Hollinger, *Acta Biomater.*, 2005, **1**, 471–84.

18 P. Zou, H. Chen, H. J. Paholak and D. Sun, *Mol. Pharm.*, 2013, **10**, 4185–94.

19 X. Dai, Z. Su and J. O. Liu, *Tetrahedron Lett.*, 2000, **41**, 6295–6298.

20 I. R. Clemitson, *Castable Polyurethane Elastomers*, CRC Press, 2008.

21 A. Prabhakar, D. K. Chattopadhyay, B. Jagadeesh and K. V. S. N. Raju, *J. Polym. Sci. Part A Polym. Chem.*, 2005, **43**, 1196–1209.

22 J. Schindelin, I. Arganda-Carreras, E. Frise, V. Kaynig, M. Longair, T. Pietzsch, S. Preibisch, C. Rueden, S. Saalfeld, B. Schmid, J.-Y. Tinevez, D. J. White, V. Hartenstein, K. Eliceiri, P. Tomancak and A. Cardona, *Nat. Methods*, 2012, **9**, 676–82.

23 P. Botella, I. Abasolo, Y. Fernández, C. Muniesa, S. Miranda, M. Quesada, J. Ruiz, S. Schwartz and A. Corma, *J. Control. Release*, 2011, **156**, 246–57.

24 J .Rocas Sorolla; P. Rocas Alonso. Process for the Manufacture of a Microencapsulated and Reactive Amphiphilic Compound, and Corresponding Microencapsulated Composition, WO2014114838 A3, 2014.

25 X. Yan, M. Delgado, A. Fu, P. Alcouffe, S. G. Gouin, E. Fleury, J. L. Katz, F. Ganachaud and J. Bernard, *Angew. Chem. Int. Ed. Engl.*, 2014, 1–5.

26 J.-W. Yoo, N. Doshi and S. Mitragotri, *Adv. Drug Deliv. Rev.*, 2011, **63**, 1247–1256.

27 K. Landfester and V. Mailänder, *Expert Opin. Drug Deliv.*, 2013, **10**, 593–609.

28 R. G. Strickley, *Pharm. Res.*, 2004, **21**, 201–30.

29 K. Landfester, N. Bechthold, F. Tiarks and M. Antonietti, *Macromolecules*, 1999, **32**, 5222–5228.

30 Peihong Ni, Mingzu Zhang and Nianxi Yan, *J. Memb. Sci.*, 1995, **103**, 51–55.

31 G. Morral-Ruíz, C. Solans, M. L. García and M. J. García-Celma, *Langmuir*, 2012, **28**, 6256–64.

32 R. Haubner, R. Gratias, B. Diefenbach, S. L. Goodman, A. Jonczyk and H. Kessler, *J. Am. Chem. Soc.*, 1996, **118**, 7461–7472.

33 Heming, A. M.; Mulqueen, P. J.; Scher, H. B.; Shirley, I. M. Use of Reactive Polymeric Surfactants in the Formation of Emulsions, US7199185 B2, 2002.

34 R. Cheng, F. Feng, F. Meng, C. Deng, J. Feijen and Z. Zhong, *J. Control. Release*, 2011, **152**, 2–12.

35 R. W. Sabnis, *Handbook of Biological Dyes and Stains: Synthesis and Industrial Applications*, 2010.

36 S. Jiwpanich, J.-H. Ryu, S. Bickerton and S. Thayumanavan, *J. Am. Chem. Soc.*, 2010, **132**, 10683–5.

37 H. Chen, S. Kim, L. Li, S. Wang, K. Park and J.-X. Cheng, *Proc. Natl. Acad. Sci.* , 2008, **105** , 6596–6601.

38 T. M. Allen and A. Chonn, *FEBS Lett.*, 1987, **223**, 42–46.

TABLE OF CONTENTS

Pau Rocas, Yolanda Fernández, Simó Schwartz Jr, Ibane Abasolo, Josep Rocas*, Fernando Albericio**

Page No.-Page No.

Multifunctionalized Polyurethane-Polyurea Nanoparticles: Hydrophobically Driven Self-Stratification at the o/w Interface Modulates Encapsulation Stability

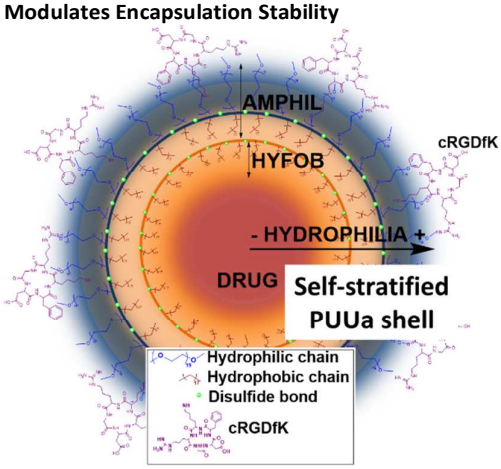

The combination of an amphiphilic and a hydrophobic reactive prepolymer promotes self-stratification of the whole PUUa NP by hydrophobic interactions.

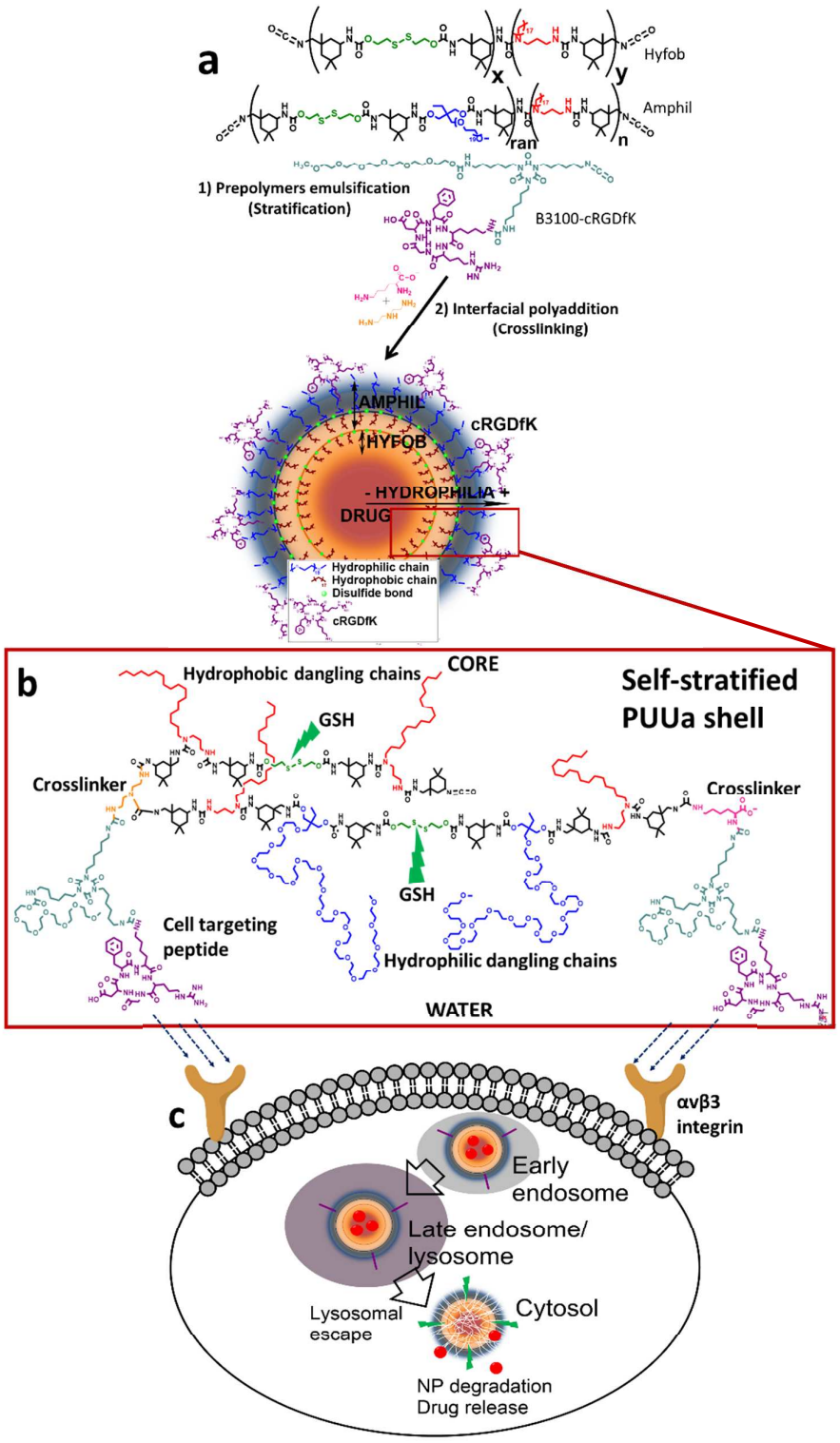

Figure 1. Schematic illustration of PUUa NPs synthesis, structure and application. After emulsification of prepolymers in water, the self-stratified shell is consolidated by a two-step interfacial crosslinking creating a robust multiwalled NP a). Dangling side-chains of functional prepolymers self-orient through the oil-water interface and drive the self-assembly by hydrophobic and hydrophilic interactions. The hydrophilic cRGDfK peptide is covalently linked via urea bonds to the more external part of the shell b). Scheme of PUUa NPs receptor mediated internalization and cytosolic delivery of hydrophobic cargo c).

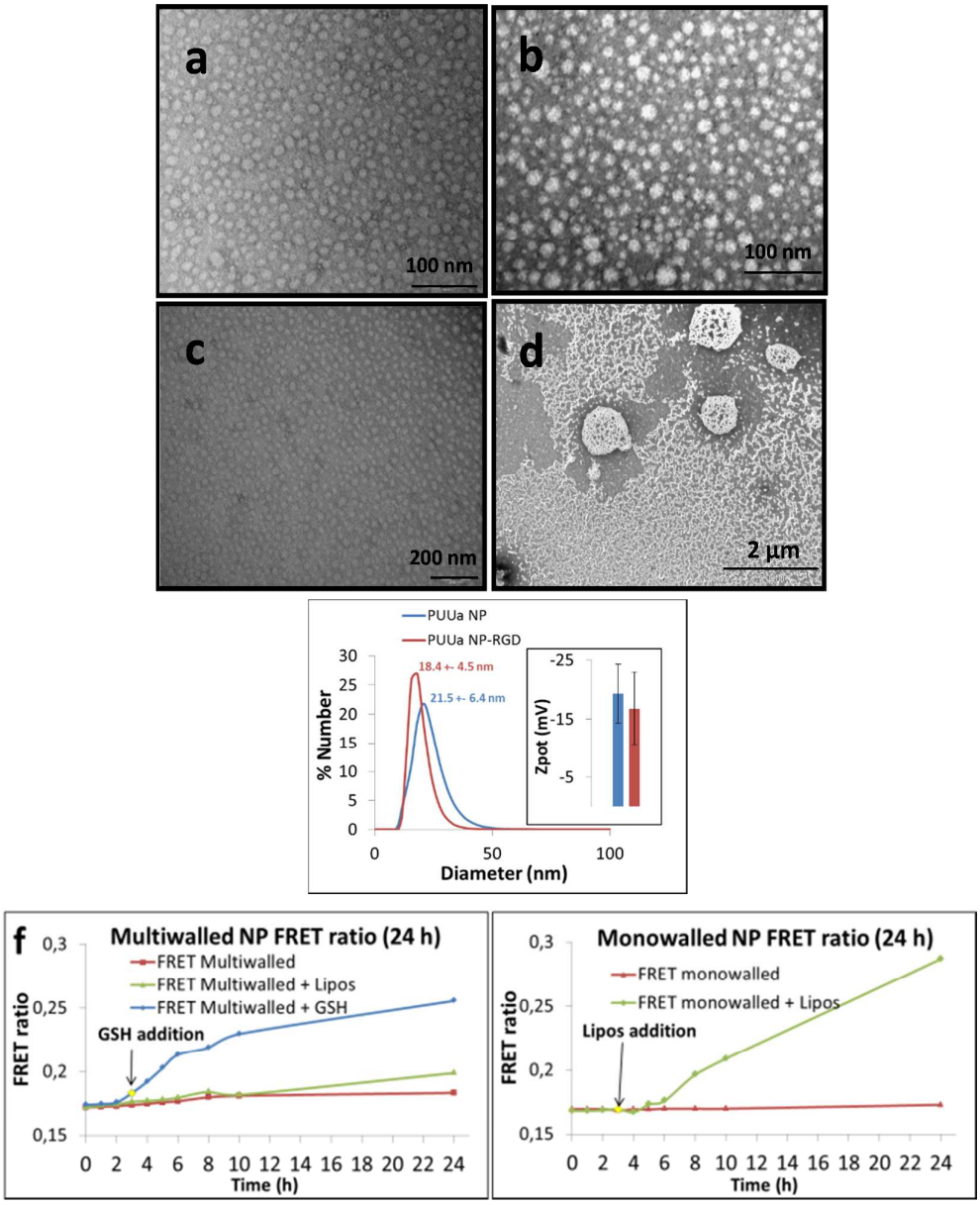

Figure 2. TEM images of multiwalled PUUa NP a) and PUUa NP-RGD b). TEM images of PUUa NPs before c) and after treatment with GSH 10 mM at 37 ºC during 24 h d). After treatment with GSH clear degradation of PUUa NPs is achieved and degraded polymers form aggregates up to 1 µm size. e) Hydrodynamic diameter by DLS and Zeta Potential of PUUa NP-RGD (blue) and PUUa NP (red). Release dynamics comparison between multiwalled and monowalled PUUa NPs f). Aqueous media (Red), *in vivo*-like media (green) and 10 mM reduced GSH (blue).

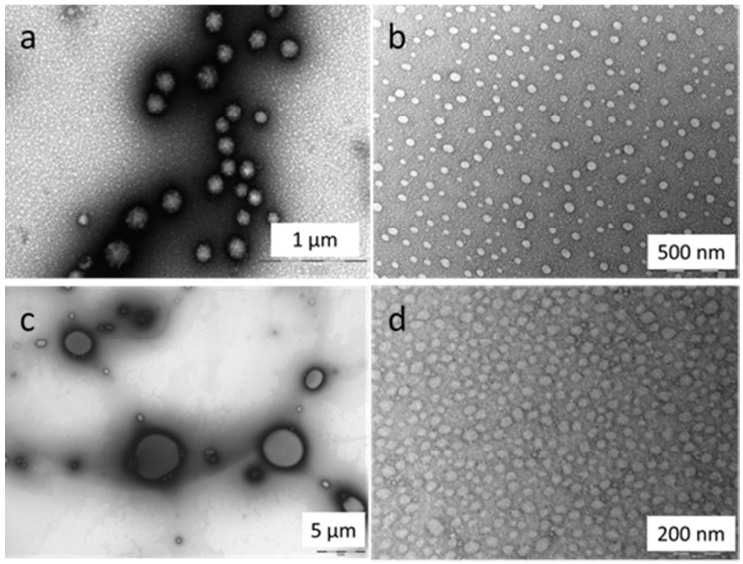

Multiwalled Samples	Diameter (nm)	SD (nm)	PDI
a) DETA-crosslinked PUUa NP	170.3	32.0	0.04
b) Lys-crosslinked PUUa NP	53.2	22.8	0.18
c) Non-crosslinked PUUa NP	207.7	590.8	5.91
d) Lys-DETA-crosslinked PUUa NP	29.0	5.0	0.03

Figure 3. TEM micrographs of multiwalled PUUa NPs showing the importance of the crosslinking process to get a monodisperse sample. After emulsification of reactive prepolymers in water PUUa NPs were crosslinked by successive additions of Lys and/or DETA, respectively a, b, d). Non-crosslinked PUUa NPs were kept under magnetic stirring during 3 days until isocyanate group disappeared from the IR spectra due to reaction with water. It can be observed that without crosslinker, NPs are not interfacially stabilized and a highly polydisperse sample is obtained c). Images were statistically analyzed by random recording of 5 different zones of the copper grid.

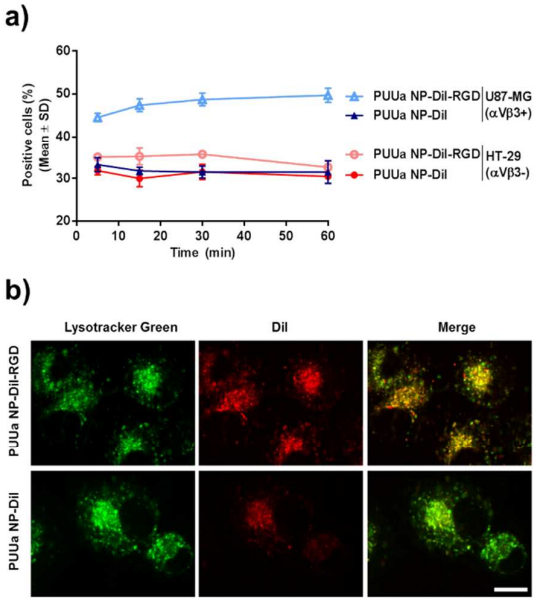

Figure 4. PUUa NP internalization. a) Flow cytometry studies were performed in U87-MG (αvβ3-positive) and HT-29 (αvβ3-negative) cancer cells at different time points with 10 µg/mL of DiI (38.5 µg/mL of NPs). b) Confocal images of U87-MG cells incubated 24 h with 1 µg/mL of DiI and stained with Lysotracker Green to show lysosomal localization of PUUa NPs. Magnification bar corresponds to 10 µm.